

A Method to Measure β_1 Using $\bar{B}^0 \rightarrow D^0 \bar{h}^0$ With Multibody Decay

Alex Bondar,¹ Tim Gershon^y,² and Pavel Krokovny^z

¹Budker Institute of Nuclear Physics, Novosibirsk

²High Energy Accelerator Research Organization (KEK), Tsukuba

Abstract

We describe a new method to measure the angle β_1 of the CKM Unitarity Triangle using amplitude analysis of the multibody decay of the neutral D meson produced via $\bar{B}^0 \rightarrow D^0 \bar{h}^0$ colour-suppressed decays. The method employs the interference between D^0 and \bar{D}^0 to directly extract the value of β_1 , and thus resolve the ambiguity between β_1 and $-\beta_1$ in the measurement of $\sin(\beta_1)$ using $\bar{B}^0 \rightarrow J/\psi K_S$. We present a feasibility study of this method using Monte Carlo simulation.

PACS numbers: 11.30.Er, 12.15.Hh, 13.25.Hw, 14.40.Nd

^a a.e.bondar@inp.nsk.su

^y gershon@mail.kek.jp

^z krokovny@mail.kek.jp

I. INTRODUCTION

Precise determinations of the Cabibbo-Kobayashi-Maskawa (CKM) matrix elements [1] are important to check the consistency of the Standard Model and search for new physics. The value of $\sin(2\beta_1)$, where β_1 is one of the angles of the Unitarity Triangle [2] is now measured with high precision: $\sin(2\beta_1) = 0.731 \pm 0.056$ [3]. However, this measurement contains an intrinsic ambiguity: $2\beta_1 \rightarrow -2\beta_1$. Various methods to resolve this ambiguity have been introduced [4], but they require very large amounts of data (some impressive first results notwithstanding [5]).

We suggest a new technique based on the analysis of $\bar{B}^0 \rightarrow D h^0$, followed by the three-body decay of the neutral D meson, $D \rightarrow K_S \pi^+$. Here we use h^0 to denote a light neutral meson, such as η^0 ; η'^0 ; η_c^0 . The modes $\bar{B}^0 \rightarrow D_{CP} h^0$, utilizing the same B decay but requiring the D meson to be reconstructed via CP eigenstates, have previously been proposed as "gold-plated" modes to search for new physics effects [6]. Such effects may result in deviations from the Standard Model prediction that CP violation effects in $b \rightarrow \bar{c} \bar{c}$ transitions should be very similar to those observed in $b \rightarrow \bar{u} \bar{d}$ transitions, such as $\bar{B}^0 \rightarrow J/\psi K_S$. Detailed considerations have shown that the contributions from $b \rightarrow \bar{u} \bar{d}$ amplitudes, which are suppressed by a factor of approximately 0.02 [7], can be taken into account [8]. Consequently, within the Standard Model, studies of $\bar{B}^0 \rightarrow D_{CP} h^0$ can give a measurement of $\sin(2\beta_1)$ that is more theoretically clean than that from $\bar{B}^0 \rightarrow J/\psi K_S$. However, these measurements still suffer from the ambiguity mentioned above.

In the case that the neutral D meson produced in $\bar{B}^0 \rightarrow D h^0$ is reconstructed in a multibody decay mode, with known decay model, the interference between the contributing amplitudes allows direct sensitivity to the phases. Thus $2\beta_1$, rather than $\sin(2\beta_1)$ is extracted, and the ambiguity $2\beta_1 \rightarrow -2\beta_1$ can be resolved. This method is similar to that used to extract β_3 , using $B \rightarrow D K$ followed by multibody D decay [9, 10]; in the β_3 analysis the ambiguities in the result are also reduced compared to more traditional techniques [11, 12]. In addition, with current B factory statistics, better precision on β_3 is obtained using multibody D decay.

There are a large number of different final states to which this method can be applied. In addition to the possibilities for h^0 , and the various different multibody D decays which can be used, the method can also be applied to $\bar{B}^0 \rightarrow D \bar{h}^0$. In this case, the usual care must be taken to distinguish between the decays $D \rightarrow D^0$ and $D \rightarrow \bar{D}$ [13].

In this paper we concentrate primarily on the decay $\bar{B}^0 \rightarrow D^0$ with $D \rightarrow K_S \pi^+$ (and denote the decay chain as $\bar{B}^0 \rightarrow (K_S \pi^+)_D \pi^0$). This multibody D decay has been shown, in the β_3 analysis, to be particularly suitable for Dalitz plot studies. In the remainder of the paper, we first give an overview of the relevant formalism, and then turn our attention to Monte Carlo simulation studies of $\bar{B}^0 \rightarrow (K_S \pi^+)_D \pi^0$. We attempt to include all experimental effects, such as background, resolution, flavour tagging, and so on, in order to test the feasibility of the method. Based on these studies, we estimate the precision with which $2\beta_1$ can be extracted with the current B factory statistics.

Before turning to the details, we note that this method can also be applied to other neutral B meson decays with a neutral D meson in the final state. In particular, the decay $\bar{B}^0 \rightarrow D K_S$ has contributions from $b \rightarrow \bar{c} \bar{c}$ and $b \rightarrow \bar{u} \bar{d}$ amplitudes, which have a relative weak phase difference of β_3 . Thus a time-dependent Dalitz plot analysis of $\bar{B}^0 \rightarrow (K_S \pi^+)_D K_S$ can be used to simultaneously measure β_1 and β_3 [14], and can test the Standard Model prediction that CP violation effects in $b \rightarrow \bar{c} \bar{c}$ transitions should be, to a

good approximation, the same as those in $b^+ \bar{b}^-$ transitions. Furthermore, modes such as $B_s^0 \bar{B}_s^0$ and $(K_S^+ \bar{K}_S^-)_D$ can in principle be used to measure the weak phase in $B_s^0 \bar{B}_s^0$ mixing. However, our feasibility study is not relevant to B_s^0 decay modes, which cannot be studied at a B factory operating at the (4S) resonance.

II. DESCRIPTION OF THE METHOD

Consider a neutral B meson, which is known to be \bar{B}^0 at time t_{tag} (for experiments operating at the (4S) resonance, such knowledge is provided by tagging the flavour of the other B meson in the (4S) $\bar{B} \bar{B}$ event). At another time t_{sig} the amplitude content of the B meson is given by [15]

$$\bar{B}^0(t) = e^{j \frac{t-t_{\text{tag}}}{\tau_B}} \bar{B}^0(t_{\text{tag}}) \cos(m(t=2)) + i \frac{p}{q} \bar{B}^0(t_{\text{tag}}) \sin(m(t=2)); \quad (1)$$

where $t = t_{\text{sig}} - t_{\text{tag}}$, τ_B is the average lifetime of the \bar{B}^0 meson, m , p and q are parameters of $\bar{B}^0 \bar{B}^0$ mixing (m gives the frequency of $\bar{B}^0 \bar{B}^0$ oscillations, while the eigenstates of the effective Hamiltonian in the $\bar{B}^0 \bar{B}^0$ system are $\beta_i = p \beta^0 i - q \bar{\beta}^0$), and we have assumed CPT invariance and neglected terms related to the $\bar{B}^0 \bar{B}^0$ lifetime difference [16]. In the following we drop the terms of $e^{j \frac{t-t_{\text{tag}}}{\tau_B}}$.

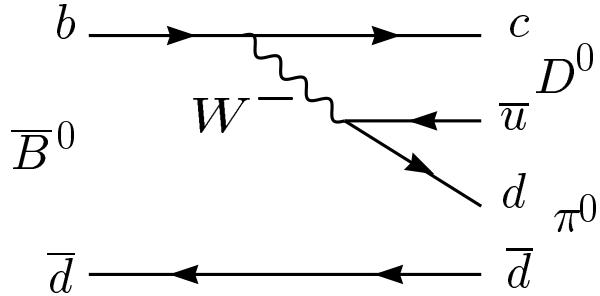


FIG. 1: Diagram for the dominant colour-suppressed amplitude for $\bar{B}^0 \rightarrow D^0$.

Let us now consider the decays of the B meson to $D h^0$. At first, we consider only the favoured $b^+ \bar{b}^-$ (and charge conjugate) amplitude, shown in Fig. 1. Then the D meson produced by B decay at time t_{sig} is given by the following admixture:

$$D_{\bar{B}^0}(t) = D^0(t_{\text{tag}}) \cos(m(t=2)) + i \frac{p}{q} h^0(t=2) \bar{D}^0(t_{\text{tag}}) \sin(m(t=2)); \quad (2)$$

where we use h^0 to denote the CP eigenvalue of h^0 , and l gives the orbital angular momentum in the $D h^0$ system [17].

The next step is the multibody decay of the D meson. We use $D^0 \rightarrow K_S^+ \bar{K}_S^-$ for illustration. We follow [9] and describe the amplitude for a \bar{D}^0 decay to this final state as $f(m_+^2; m_-^2)$, where m_+^2 and m_-^2 are the squares of two body invariant masses of the K_S^+ and K_S^- combinations. Assuming no CP violation in the neutral D meson system, the amplitude for a D^0 decay is then given by $f(m^2; m_+^2)$. The amplitude for the B decay at

time t_{sig} is then given by

$$M_{\bar{B}^0}(t) = f(m^2; m_+^2) \cos(m t=2) - i \frac{p}{q} h^0(-1)^1 f(m_+^2; m^2) \sin(m t=2); \quad (3)$$

Similar expressions for a state which is known to be B^0 at time t_{tag} are obtained by interchanging $B^0 \leftrightarrow \bar{B}^0$, $D^0 \leftrightarrow \bar{D}^0$, $p \leftrightarrow q$ and $m_+^2 \leftrightarrow m^2$:

$$B^0(t) = e^{i t \frac{p}{q} h^0} \bar{B}^0 \cos(m t=2) - i \frac{q}{p} \bar{B}^0 \sin(m t=2); \quad (4)$$

$$\bar{D}^0(t) = \bar{D}^0 \cos(m t=2) - i \frac{q}{p} h^0(-1)^1 D^0 \sin(m t=2); \quad (5)$$

$$M_{B^0}(t) = f(m_+^2; m^2) \cos(m t=2) - i \frac{q}{p} h^0(-1)^1 f(m^2; m_+^2) \sin(m t=2); \quad (6)$$

In the Standard Model, $q \bar{p} p \bar{q} = 1$ to a good approximation, and, in the usual phase convention, $\arg(q \bar{p} p \bar{q}) = 2\pi$. Then

$$M_{\bar{B}^0}(t) = f(m^2; m_+^2) \cos(m t=2) - i e^{i 2\pi} h^0(-1)^1 f(m_+^2; m^2) \sin(m t=2); \quad (7)$$

$$M_{B^0}(t) = f(m_+^2; m^2) \cos(m t=2) - i e^{+i 2\pi} h^0(-1)^1 f(m^2; m_+^2) \sin(m t=2); \quad (8)$$

and it can be seen that once the model $f(m_+^2; m^2)$ is fixed, the phase 2π can be extracted from a time-dependent Dalitz plot fit to B^0 and \bar{B}^0 data.

At this point it is instructive to compare to the $B \rightarrow D K$ analysis [9]. In that case we obtained time-independent expressions

$$M_B = f(m^2; m_+^2) + r_{D K} e^{i(\Delta \phi - \pi)} f(m_+^2; m^2); \quad (9)$$

$$M_{B^+} = f(m_+^2; m^2) + r_{D K} e^{i(\Delta \phi + \pi)} f(m^2; m_+^2); \quad (10)$$

where $r_{D K}$ is the ratio of the magnitudes of the contributing (suppressed and favoured) decay amplitudes ($r_{D K} = A(B \rightarrow \bar{D}^0 K) / A(B \rightarrow D^0 K)$), and $\Delta \phi$ is the strong phase between them. It can be seen that the role of $r_{D K}$ in the time-independent analysis is taken by the expression $\tan(m t=2)$ in the time-dependent case. Furthermore, in the time-dependent case, there is no non-trivial strong phase difference. Therefore, the time-dependent analysis has the advantage that there is only one unknown parameter, which partly compensates for the experimental disadvantages that are accrued.

We now consider the effect of the Cabibbo-suppressed $b \rightarrow u \bar{d}$ amplitudes, shown in Fig. 2. The magnitude of this amplitude is expected to be smaller than the Cabibbo-favoured diagram (Fig. 1) by a factor of

$$r_{D^0} = \frac{A(\bar{B}^0 \rightarrow \bar{D}^0 \bar{D}^0)}{A(\bar{B}^0 \rightarrow D^0 D^0)} \frac{V_{ub} V_{cd}}{V_{cb} V_{ud}} \approx 0.02; \quad (11)$$

Since this simple approximation neglects hadronic factors, it is the same for all h^0 , though the precise values will depend on the final state. We denote the strong phase difference between the two amplitudes as $\Delta \phi$ (which, in general, will be different for each h^0). Including this

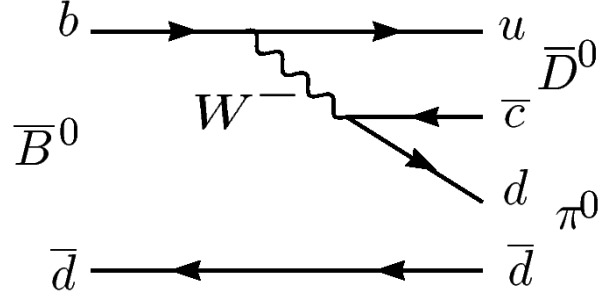


FIG. 2: Diagram for the colour- and Cabibbo-suppressed amplitude for $\bar{B}^0 \rightarrow D^0 \bar{D}^0$.

amplitude, the expressions Eqs. 7 and 8 are replaced by

$$M_{\bar{B}^0}(t) = \frac{h}{f(m^2; m_+^2) + r_{D^0} e^{i(\Delta_0 - \Delta_3)} f(m_+^2; m^2)} \cos(m t/2) \quad (12)$$

$$+ i e^{i 2 \Delta_1 - h_0} (-1)^1 \frac{h}{f(m_+^2; m^2) + r_{D^0} e^{i(\Delta_0 + \Delta_3)} f(m_+^2; m^2)} \sin(m t/2);$$

$$M_{B^0}(t) = \frac{h}{f(m_+^2; m^2) + r_{D^0} e^{i(\Delta_0 + \Delta_3)} f(m_+^2; m^2)} \cos(m t/2) \quad (13)$$

$$+ i e^{+ i 2 \Delta_1 - h_0} (-1)^1 \frac{h}{f(m^2; m_+^2) + r_{D^0} e^{i(\Delta_0 - \Delta_3)} f(m^2; m_+^2)} \sin(m t/2);$$

In principle, therefore, it is possible to extract all four unknown parameters $(\Delta_1; r_{D^0}; \Delta_0; \Delta_3)$ from the time-dependence of the Dalitz plot. However, due to the smallness of r_{D^0} , this is highly impractical. On the other hand, the above formulation allows us to generate simulated data including the suppressed contribution, and thus estimate the effect of its neglect.

Again, we note that in the case of $\bar{B}^0 \rightarrow D K_S$, the ratio of amplitudes is not small ($r_{D K_S} \approx 0.4$), and in this case both Δ_1 and Δ_3 can be extracted from a time-dependent Dalitz plot analysis. In fact, the size of $r_{D K_S}$ makes this mode quite attractive for the measurement of Δ_3 . Similarly, a time-independent analysis can be performed using $\bar{B}^0 \rightarrow D \bar{K}^0$, with $K^0 \rightarrow K^+ K^-$, but in this case additional uncertainty arises due to possible contributions from nonresonant $\bar{B}^0 \rightarrow D K^+$ [18].

III. FEASIBILITY STUDY

The potential accuracy of the Δ_1 determination is estimated using a Monte Carlo based feasibility study. We generate $\bar{B}^0 \rightarrow (K_S^+ K_S^-)_D h^0$ decays and process the events with detector simulation and reconstruction. Signal and background candidates are selected. Signal and tagging B vertexes are reconstructed in order to obtain t , and the flavour of the tagging B meson is obtained. Finally, we perform an unbinned likelihood fit of the time-dependent Dalitz plot to obtain the value of Δ_1 and its uncertainty.

A. Monte Carlo Generation

In order to test the feasibility of the method described above, we have developed an algorithm to generate Monte Carlo simulated data, based on EvtGen [19]. We first test the generator by restricting the $D \rightarrow K_S^+ K_S^-$ decay to the K_S^0 channel. In this case,

the formalism simplifies to the familiar $D_{CP}h^0$ case, and the time-dependent decay rate (neglecting suppressed amplitudes), is given by

$$P(t) = \frac{e^{i t \frac{q}{m_B} B_0}}{4 B_0} f_1 + q S_{D_{CP}h^0} \sin(m_B t) g; \quad (14)$$

where the bavour charge q is $+1$ (-1) when the tagging B meson is B^0 (\bar{B}^0), and, within the Standard Model, $S_{D_{CP}h^0} = S_{D_{CP}h^0}(-1)^1 \sin(2\pi_1)$. For the CP odd decay $D^+ \rightarrow K_S^0 h^0$, $S_{D_{CP}h^0} = 1$, so for $(K_S^0)_D h^0$, $S_{D_{CP}h^0} = \sin(2\pi_1)$. Fig. 3 shows generator level information for these decays.

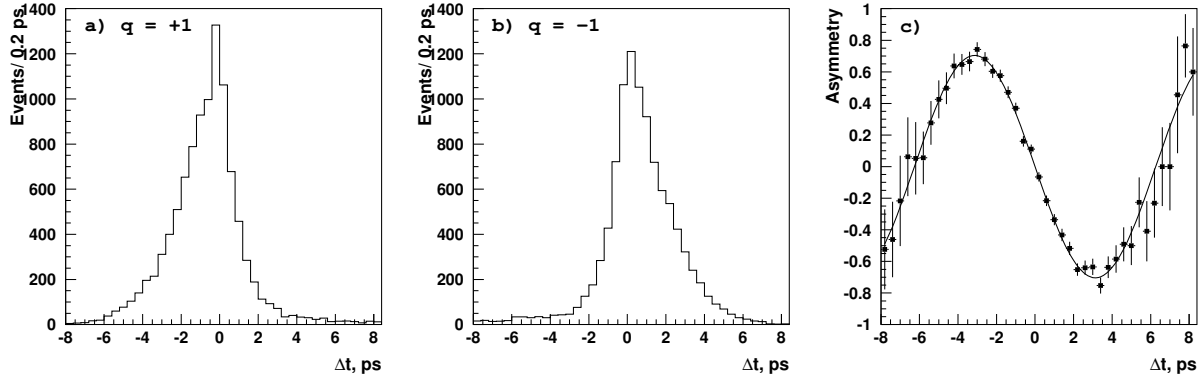


FIG. 3: t distributions for $\bar{B}^0 \rightarrow (K_S^+)_D h^0$ (a) $q = +1$, (b) $q = -1$, (c) asymmetry.

We next implement three body D decays into our generator. The amplitude of the $\bar{D}^0 \rightarrow K_S^+ h^0$ decay is described by a coherent sum of two-body decay amplitudes plus non-resonant part:

$$f(m_{K_S^+}^2; m_{K_S^+}^2) = \sum_{j=1}^N a_j e^{i \phi_j} A_j(m_{K_S^+}^2; m_{K_S^+}^2) + b e^{i \phi}; \quad (15)$$

where N is the number of resonances, $A_j(m_{K_S^+}^2; m_{K_S^+}^2)$, a_j and ϕ_j are the matrix element, amplitude and phase, respectively, for the j -th resonance, and b and ϕ are the amplitude and phase for the non-resonant component. For further details, see [9] and references therein. Table I describes the set of resonances we use in the decay model of our generator, which is similar to that in the CLEO measurement [20]. Fig. 4 shows the Dalitz plot distribution for the $\bar{D}^0 \rightarrow K_S^+ h^0$ decay generated according this model.

For further confirmation of the operation of our generator, we look at the generator level time-dependent Dalitz plot. We generate $\bar{B}^0 \rightarrow (K_S^+)_D h^0$ decays using $2\pi_1 = 47^\circ$. In Fig. 5 we show the invariant mass distributions of the D decay daughters for events with $q = +1$, and compare those for events with t greater than $B_0 = 2$ with those for events with t less than $B_0 = 2$. Events with $|t| < B_0 = 2$ or $q = +1$ are not shown. We see clear differences in the two invariant mass distributions; in particular we see more events with positive than negative t in the h^0 region of the K_S^+ invariant mass distribution, as expected from Fig. 3.

Since we are concerned with the feasibility of studying these modes at B factory experiments, we use the software of the Belle collaboration to perform simulation of the Belle

TABLE I: List of resonances used for $\bar{D}^0 \rightarrow K_S^+ \pi^-$ decay simulation.

Resonance	Amplitude	Phase (°)
$K^*(892)^+$	1.418	170
$K_0(1430)^+$	1.818	23
$K_2(1430)^+$	0.909	194
$K^*(892)^+ (DCS)$	0.100	341
K_S^0	0.909	20
$K_S^+ (f_0)$	0.034	134
$K_S f_0(980)$	0.309	208
$K_S f_0(1370)$	1.636	105
$K_S f_2(1270)$	0.636	328
$K_S^+ \text{ non-resonant}$	1.0	0

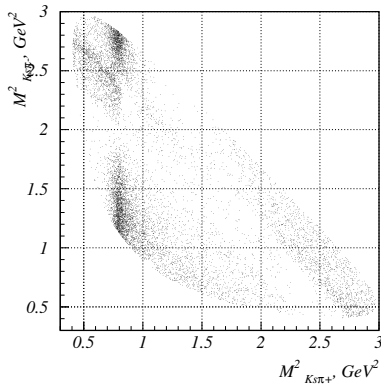


FIG. 4: $\bar{D}^0 \rightarrow K_S^+ \pi^-$ decay Dalitz plot.

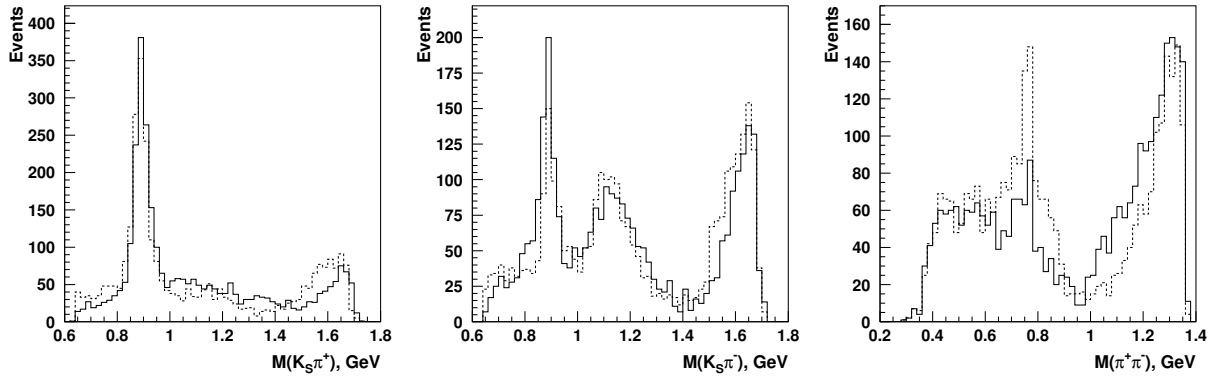


FIG. 5: Generator level invariant mass distributions of D decay daughters produced in the $\bar{B}^0 \rightarrow K_S^+ \pi^-$ decay chain. Events are generated with $\theta_1 = 47^\circ$, and only events with $q = 1$ (tagging B decays as \bar{B}^0) are shown. The dashed histograms show distributions for events with $t > B^0 = 2$, the solid histograms show those for events with $t < B^0 = 2$.

detector and to reconstruct candidate events. The Belle detector is a large-solid-angle magnetic spectrometer that consists of a silicon vertex detector (SVD), a central drift chamber (CDC), aerogel threshold Cerenkov counters (ACC), time-of-light scintillation counters (TOF), and an electromagnetic calorimeter (ECL) located inside a superconducting solenoid coil that provides a 1.5 T magnetic field. An iron flux-return located outside of the coil is instrumented to detect K_L^0 mesons and to identify muons (KLM). The detector is described in detail elsewhere [21]. The detector simulation is based on GEANT [22]. Belle is installed at the interaction point of the KEKB asymmetric-energy e^+e^- (3.5 GeV on 8 GeV) collider [23]. KEKB operates at the $(4S)$ resonance ($\sqrt{s} = 10.58$ GeV) with a peak luminosity that exceeds $1.5 \times 10^{34} \text{ cm}^{-2} \text{ s}^{-1}$. The asymmetric energy allows it to be determined from the displacement between the signal and tagging B meson decay vertices.

B. Event Reconstruction

We reconstruct the decays $\bar{B}^0 \rightarrow (K_S^+ \pi^-)_D h^0$ for $h^0 = \pi^0$; and η . We use the subdecays $K_S^+ \rightarrow \pi^+ \pi^0$, $\eta \rightarrow \pi^+ \pi^0 \pi^0$, and $\eta \rightarrow \pi^+ \pi^0 \pi^0$. The reconstruction, including suppression of the dominant background from $e^+e^- \rightarrow q\bar{q}$ ($q = u; d; s; c$) continuum processes, is highly similar to that in related Belle analyses [24]. The properties of the background events are studied using generic $B\bar{B}$ and $q\bar{q}$ Monte Carlo. Our studies allow us to estimate the number of signal and background events to expect from a given data sample (we use the data sample of 253 fb^{-1} , containing 275 million $B\bar{B}$ pairs, collected with the Belle detector before summer 2004 as our baseline). The results are summarized in Table II.

TABLE II: Detection efficiency, expected numbers of signal (N_{sig}) and background (N_{bkg}) events and signal purity for the $\bar{B}^0 \rightarrow (K_S^+ \pi^-)_D h^0$ final states. The expected numbers of events are based on the Belle data sample of 253 fb^{-1} .

Process	Efficiency (%)	N_{sig}	N_{bkg}	Purity
D^0	8.1	118	49	71%
D^+	3.9	49	8	86%
D^-	4.3	47	15	76%
Sum		214	72	75%

For our further studies, we use only the D^0 mode, for which the expected number of signal events is the largest. In our pseudo-experiments, described below, we use numbers of signal and background events (300 and 100 respectively) which are rounded up from the totals in Table II, as we expect some improvement is possible due to optimization of the selection for this analysis.

The signal B meson decay vertex is reconstructed using the D trajectory and an interaction profile (IP) constraint. The tagging B vertex position is obtained with the IP constraint and with well reconstructed tracks that are not assigned to signal B candidate. The algorithm is described in detail elsewhere [25].

Tracks that are not associated with the reconstructed $\bar{B}^0 \rightarrow (K_S^+ \pi^-)_D h^0$ decay are used to identify the flavour of the accompanying B meson. The tagging algorithm is described in detail elsewhere [26]. We use two parameters, q and r , to represent the tagging information. The first, q , has the discrete value +1 (−1) when the tagging B meson is more

likely to be a B^0 (\bar{B}^0). The parameter r corresponds to an event-by-event flavour-tagging dilution that ranges from $r = 0$ for no flavour discrimination to $r = 1$ for an unambiguous flavour assignment.

We divide the $t_1 = [0 : 180]$ range into 18 points in steps of 10. For each point we perform 30 pseudo-experiments with data samples consisting of 300 reconstructed D^0 events. We add 100 background events to each sample, where the background is modelled by $B^0 \rightarrow D^0 h^0$, with uniform phase space decay $\bar{D}^0 \rightarrow K_S \pi^+$.

For each pseudo-experiment, we perform an unbinned time-dependent Dalitz plot t . The inverse logarithm of the unbinned likelihood function is minimized:

$$2 \log L = \frac{1}{2^4} \sum_{i=1}^n \log p(m_{+i}^2; m_{-i}^2; t_i) - \log \int_0^{\infty} p(m_{+i}^2; m_{-i}^2; t) dm_{+i}^2 dm_{-i}^2 dt^5; \quad (16)$$

where n is the number of events, m_{+i}^2 , m_{-i}^2 and t_i are the measured invariant masses of the D daughters, and the time difference between signal and tagging B meson decays. The function $p(m_{+i}^2; m_{-i}^2; t)$ is the time-dependent Dalitz plot density, which is based on Eqs. 7 and 8, including experimental effects such as mistagging and t resolution – we use the standard Belle algorithm to take these effects into account. The background component is also introduced into p .

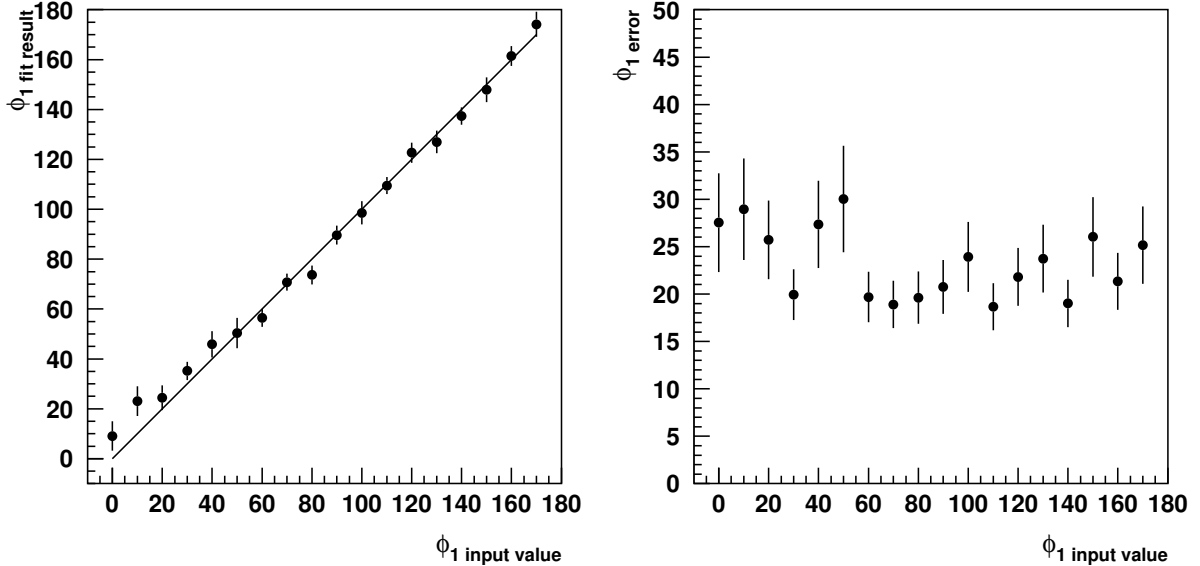


FIG. 6: (Left) average ϕ_1 fit result and (right) ϕ_1 statistical error, as functions of the input value.

Thus, for each input value of ϕ_1 we obtain fitted results from 30 pseudo-experiments. From the means and widths of the distributions of these results we obtain the average ϕ_1 fit results and estimates of their statistical errors. These results are shown in Fig. 6. We find the fit results are in good agreement with the input values, and the expected uncertainty on ϕ_1 is around 25.

To look for tails in the distributions, we also study larger ensembles of pseudo-experiments for two ϕ_1 input values: 23.5 and 66.5, which correspond to $\sin(2\phi_1) = 0.73$. We have performed this study both for the numbers of events described above, corresponding roughly

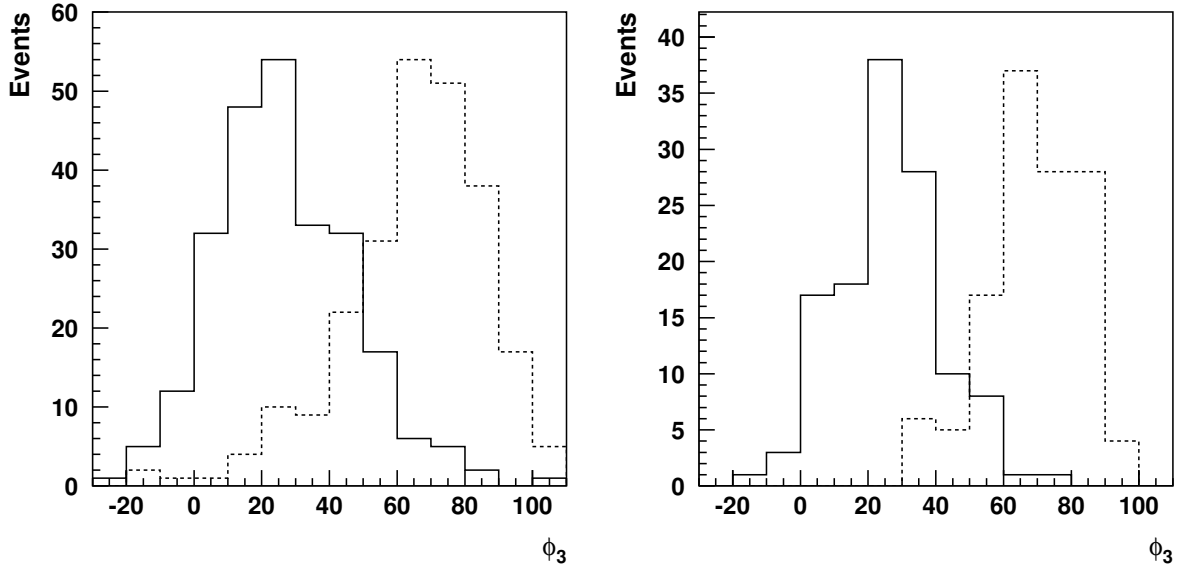


FIG. 7: Fit results for ϕ_1 . The solid (hatched) histogram corresponds to the input value $2_1 = 47$ ($2_1 = 133$). The left (right) plot corresponds to a data sample roughly equivalent to 250 fb^{-1} (500 fb^{-1}).

to 250 fb^{-1} (for which we perform 250 pseudo-experiments for each input value of ϕ_1), and for numbers twice larger (hence 500 fb^{-1} , for which we perform 125 pseudo-experiments). Fig. 7 shows the distribution of the ϕ_1 results. We do not observe any pathological behaviour, demonstrating that this method can indeed be used to distinguish the two solutions for $\sin(\phi_1)$ with sufficiently large data samples.

We have tested for possible bias in the method due to neglect of the suppressed amplitudes (Eqs. 12 and 13). Due to the smallness of r_D compared to the $B^0 \bar{B}^0$ mixing effect, we expect any such bias to be small, and indeed we find it to be smaller than 1%.

As noted above, this method is highly similar to that used to extract ϕ_3 , using $B^0 \bar{B}^0$ D K followed by multibody D decay [9, 10]. A significant complication arises in that case due to uncertainty in the D decay model, and we expect this will also affect the $B^0 \bar{B}^0 \rightarrow D^0 \bar{D}^0$ analysis. However, the time-dependent analysis does not suffer due to the smallness of the ratio of amplitudes, and therefore we expect that the model uncertainty may be smaller. Furthermore, a number of methods have been proposed to address the model uncertainty (for example, using information from CP tagged D mesons which can be studied at a factory, such as CLEO-c), and this analysis can also take advantage of any progress in that area.

IV. CONCLUSION

We have presented a new method to measure the Unitarity Triangle angle ϕ_1 using amplitude analysis of the multibody decay of the neutral D meson produced in the processes $B^0 \bar{B}^0 \rightarrow D^0 \bar{D}^0$. The method is directly sensitive to the value of 2_1 and can thus be used to resolve the discrete ambiguity $2_1 = 47^\circ \pm 180^\circ$. The expected precision of this method has been studied using Monte Carlo simulation. We expect the uncertainty on ϕ_1 to be about

25 for an analysis using a data sample of 253 fb^{-1} .

Acknowledgments

We are grateful to our colleagues in the Belle Collaboration, on whose software our feasibility study is based. We thank A. Poluektov for his help with details of the Dalitz analysis, and T. Browder and Y. Sakai for useful suggestions. We thank Y. Grossman and A. Soni for interesting discussions.

[1] M. Kobayashi and T. M. Maskawa, *Prog. Theor. Phys.* **49**, 652 (1973); N. Cabibbo, *Phys. Rev. Lett.* **10**, 531 (1963).

[2] For a review of CP violation phenomenology, see D. Kirkby and Y. Nir in S. Eidelman et al., *Phys. Lett. B* **592**, 1 (2004).

[3] B. Aubert et al. (BaBar Collaboration), hep-ex/0408127, submitted to *Phys. Rev. Lett.*; K. Abe et al. (Belle Collaboration), hep-ex/0408111, submitted to *Phys. Rev. D*.

[4] Ya. A. Zinov'ev et al., *JETP Lett.* **50**, 447 (1989), *Phys. Rev. D* **42**, 3705 (1990), *Z. Phys. A* **356**, 437 (1997); B. Kayser, hep-ph/9709382; H. R. Quinn, T. Schietinger, J. P. Silva, A. E. Snyder, *Phys. Rev. Lett.* **85**, 5284 (2000); Yu. Grossman, H. Quinn, *Phys. Rev. D* **56**, 7259 (1997); J. Charles, A. Le Yaouanc, L. Oliver, O. Pene, J.-C. Raynal, *Phys. Lett. B* **425**, 375 (1998); Erratum -ibid. B **433**, 441 (1998); T. E. Browder, A. Datta, P. J. O'Donnell, S. Pakvasa, *Phys. Rev. D* **61**, 054009 (2000); J. Charles, A. Le Yaouanc, L. Oliver, O. Pene, J.-C. Raynal, *Phys. Rev. D* **58**, 114021 (1998). See also [5] and references therein.

[5] B. Aubert et al. (BaBar Collaboration), hep-ex/0411016, submitted to *Phys. Rev. D*.

[6] Yu. Grossman, M. P. W. Morath, *Phys. Lett. B* **395**, 241 (1997).

[7] D. A. Suprun, C.-W. Chiang and J. L. Rosner, *Phys. Rev. D* **65**, 054025 (2002).

[8] R. Fleischer, *Phys. Lett. B* **562**, 234 (2003); *Nucl. Phys. B* **659**, 321 (2003).

[9] A. Poluektov et al. (Belle Collaboration), *Phys. Rev. D* **70**, 072003 (2004).

[10] A. Giri, Y. Grossman, A. Soni and J. Zupan, *Phys. Rev. D* **68**, 054018 (2003);

[11] M. Gronau and D. London, *Phys. Lett. B* **253**, 483 (1991), M. Gronau and D. W. Yeler, *Phys. Lett. B* **265**, 172 (1991).

[12] D. Atwood, I. Dunietz, and A. Soni, *Phys. Rev. Lett.* **78**, 3257 (1997), *Phys. Rev. D* **63**, 036005 (2001).

[13] A. Bondar and T. Gershon, *Phys. Rev. D* **70**, 091503(R) (2004).

[14] This has previously been noted in D. Atwood and A. Soni, *Phys. Rev. D* **68**, 033009 (2003), and in M. Gronau, Y. Grossman, N. Shuhmacher, A. Soni and J. Zupan, *Phys. Rev. D* **69**, 113003 (2004).

[15] Details of the time-evolution of the neutral B meson system can be found in many references, for example the BaBar Physics Book, P. F. Harrison and H. R. Quinn, ed., SLAC-R-0504 (1998).

[16] A full treatment of the B_s case must take the non-zero lifetime difference into account. We do not include this extension here, for brevity.

[17] In the case of $\bar{B}^0 \rightarrow D^+ h^0$, an additional factor arises due to the CP properties of the particle emitted in the D^+ decay (either $D^+ \rightarrow D^0 \pi^+$ or $D^+ \rightarrow D^0 \eta$).

[18] K. Abe et al. (Belle Collaboration), BELLE-C0NF-0502, in preparation.

- [19] EvtGen homepage: <http://www.slac.stanford.edu/lange/EvtGen/>
- [20] H. M uramatsu et al. (CLEO Collaboration), Phys. Rev. Lett. 89, 251802 (2002); Erratum – ibid: 90, 059901 (2003).
- [21] A. A bashian et al., Nucl. Instr. and Meth. A 479, 117 (2002).
- [22] R. Brun et al., GEANT 3.21, CERN Report DD/EE/84-1, 1984.
- [23] S. K urokawa and E. K ikutani, Nucl. Instr. and. Meth. A 499, 1 (2003), and other papers included in this volume.
- [24] K. Abe, et al. (Belle Collaboration), Phys. Rev. Lett. 88, 052002 (2002); K. Abe, et al. (Belle Collaboration), BELLE-CONF-0416, hep-ex/0409004.
- [25] H. Tajima et al., Nucl. Instrum. Methods Phys. Res., Sect. A 533, 370 (2004).
- [26] H. Kakuno et al., Nucl. Instrum. Methods Phys. Res., Sect. A 533, 516 (2004).